UMP kinase from *Mycobacterium tuberculosis*: Mode of action and allosteric interactions, and their likely role in pyrimidine metabolism regulation ☆

Diana C. Rostirolla [a,b], Ardala Breda [a,b], Leonardo A. Rosado [a,c], Mario S. Palma [d], Luiz A. Basso [a,b,*], Diógenes S. Santos [a,b,*]

[a] *Centro de Pesquisas em Biologia Molecular e Funcional (CPBMF), Instituto Nacional de Ciência e Tecnologia em Tuberculose (INCT-TB), Pontifícia Universidade Católica do Rio Grande do Sul (PUCRS), Av. Ipiranga 6681 – Tecnopuc – Prédio 92-A, Porto Alegre 90619-900, RS, Brazil*
[b] *Programa de Pós-Graduação em Biologia Celular e Molecular, Pontifícia Universidade Católica do Rio Grande do Sul (PUCRS), Porto Alegre, RS, Brazil*
[c] *Programa de Pós-Graduação em Medicina e Ciências da Saúde, PUCRS, Av. Ipiranga 6681, Porto Alegre 90619-900, RS, Brazil*
[d] *Laboratório de Biologia Estrutural e Zooquímica, Centro de Estudos de Insetos Sociais, Departamento de Biologia, Instituto de Biociências de Rio Claro, Universidade Estadual Paulista (UNESP), Rio Claro, SP, Brazil*

ARTICLE INFO

ABSTRACT

The *pyrH*-encoded uridine 5′-monophosphate kinase (UMPK) is involved in both *de novo* and salvage synthesis of DNA and RNA precursors. Here we describe *Mycobacterium tuberculosis* UMPK (*Mt*UMPK) cloning and expression in *Escherichia coli*. N-terminal amino acid sequencing and electrospray ionization mass spectrometry analyses confirmed the identity of homogeneous *Mt*UMPK. *Mt*UMPK catalyzed the phosphorylation of UMP to UDP, using ATP–Mg^{2+} as phosphate donor. Size exclusion chromatography showed that the protein is a homotetramer. Kinetic studies revealed that *Mt*UMPK exhibits cooperative kinetics towards ATP and undergoes allosteric regulation. GTP and UTP are, respectively, positive and negative effectors, maintaining the balance of purine versus pyrimidine synthesis. Initial velocity studies and substrate(s) binding measured by isothermal titration calorimetry suggested that catalysis proceeds by a sequential ordered mechanism, in which ATP binds first followed by UMP binding, and release of products is random. As *Mt*UMPK does not resemble its eukaryotic counterparts, specific inhibitors could be designed to be tested as antitubercular agents.

Introduction

Human tuberculosis (TB),[1] mainly caused by *Mycobacterium tuberculosis*, is a major cause of illness and death worldwide. *M. tuberculosis* is a remarkably successful pathogen that latently infects one third of the world population [1] and, despite the availability of effective chemotherapy and moderately protective vaccine,

the tubercle bacillus continues to claim more lives than any other single infectious agent [2]. Increasing HIV–TB co-infections [2], the emergence of multidrug-resistant (MDR), extensively drug-resistant (XDR) [3], and, more recently, of totally drug-resistant strains (TDR) [4] have highlighted the need for the development of new therapeutic strategies to combat TB. Strategies based on the discovery of new targets for antimycobacterial agent development include elucidation of

the role played by proteins of essential and, preferentially, exclusive biochemical pathways for mycobacterial growth [5].

Rational inhibitor design relies on mechanistic and structural information on the target enzyme. Enzyme inhibitors make up roughly 25% of the drugs marketed in United States [6]. Enzymes offer unique opportunities for drug design that are not available to cell surface receptors, nuclear hormone receptors, ion channel, transporters, and DNA [6]. It has been pointed out that one of the lessons to be learned from marketed enzyme inhibitors is that the most potent and effective inhibitors take advantage of enzyme chemistry to achieve inhibition [7]. Moreover, the recognition of the limitations of high-throughput screening approaches in the discovery of candidate drugs has rekindled interest in rational de-sign methods [8]. Accordingly, mechanistic analysis should always be a top priority for enzyme-targeted drug programs aiming at the rational design of potent enzyme inhibitors.

Nucleotides are important molecules present in all living organisms as they constitute the building blocks for nucleic acids and also serve as energy sources for many biochemical reactions [9]. Pyrimidine nucleotides can be synthesized by de novo and salvage pathways resulting in a common product, the nucleotide uridine 5′-monophosphate (UMP) [10]. Subsequent phosphorylation of UMP yields UDP that leads to the synthesis of all other pyrimidine nucleotides [11]. Nucleoside monophosphate (NMP) kinases play an important role in the biosynthesis of nucleotides and represent a homogeneous family of catalysts related to adenylate kinase (EC 2.7.4.3). They catalyze the synthesis of nucleoside diphosphates (NDPs), which will be converted to nucleoside triphosphates (NTPs) by a non-specific nucleoside diphosphate kinase [12]. UMP kinases (UMPKs) catalyze the reversible transfer of the γ-phosphoryl group from ATP to UMP in the presence of a divalent cation, usually Mg^{2+} (Fig. 1) [13]. In general, eukaryotic UMP/CMP kinases (EC 2.7.4.14) are monomers, phosphorylate with comparable efficiency both UMP and CMP, and are structurally similar to other NMP kinases (such as adenylate kinase) [12,14–16]. In contrast, bacterial UMPKs (EC 2.7.4.22) are specific for UMP, exist in solution as stable homohexamers, and do not resemble either UMP/CMP kinases or NMP kinases from other organisms based on sequence comparisons [17,18]. Kinetic studies have shown that bacterial UMPKs can be activated by GTP and/or be subject to feed-back inhibition by UTP, the major product of the reaction they cat-alyze [17–21], regulating the balance of purine versus pyrimidine nucleoside triphosphates synthesis [13].

As pyrimidine biosynthesis is an essential step in the progres-sion of TB, enzymes of this pathway are attractive antitubercular drug targets [22]. Homologs to enzymes in the pyrimidine pathway have been identified in the genome sequence of M. tuberculosis [23]. A rapid recombination method for screening and confirma-tion of gene essentiality has recently been proposed to allow identification of which of the approximately 4000 genes of M. tuberculosis are worthy of further study as drug targets [24]. The product of pyrH (Rv2883) gene has been shown to be essential for M. tuberculosis growth by the rapid screening method [24].
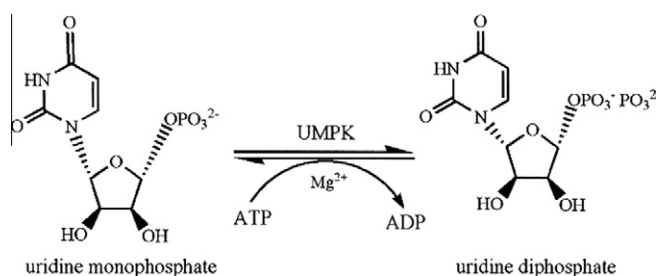
Genetic studies have provided evidence that UMPK is essential for growth in both Gram-negative (Escherichia coli) [25,26] and Gram-positive bacteria (Streptococcus pneumoniae) [19]. Although the pyrH gene has been proposed by sequence homology to encode a UMPK protein [23], there has been no formal biochemical proof as to ascertain the correct assignment to the open reading frame of pyrH gene in M. tuberculosis.

In the present work, the pyrH gene from M. tuberculosis strain H37Rv was PCR amplified, cloned, and recombinant UMPK (MtUMPK) was purified to homogeneity. N-terminal amino acid sequencing and electrospray ionization mass spectrometry (ESI-MS) analyses were carried out to confirm the identity of the recom-binant MtUMPK protein. Initial velocity studies were performed to evaluate the kinetic parameters of the recombinant MtUMPK. In addition, isothermal titration calorimetry study of substrates bind-ing was carried out to demonstrate the order of substrate addition in the kinetic mechanism of MtUMPK. Protein allosteric regulation by ATP, GTP, and UTP have also been demonstrated. These results represent an important step for the rational design of MtUMPK inhibitors that can further be tested as anti-TB drugs.

Materials and methods

Amplification, cloning and DNA sequencing of the pyrH gene

The full-length pyrH (Rv2883c) coding region [23] was PCR amplified using the genomic DNA from M. tuberculosis H37Rv as template and a high fidelity proof-reading thermostable DNA poly-merase (Pfu® DNA polymerase, Stratagene). The synthetic oligonu-cleotides used (forward primer, 5′-GT<u>C</u> ATA T<u>GA</u> CAG AGC CCG ATG TCG CCG GC-3′; and reverse primer, 5′-TA<u>A</u> AGC T<u>TT</u> CAG GTG GTG ACC AGC GTT CCG A-3′) were designed to contain, respectively, NdeI and HindIII (New England Biolabs) restriction sites (under-lined). Dimethyl sulfoxide (DMSO) was added to a final concentra-tion of 10%. The 786-bp amplicon was detected on 1% agarose gel and purified utilizing the Quick Gel Extraction kit (Invitrogen). The PCR fragment was cloned into pCR-Blunt® vector (Invitrogen) and, following transformation of E. coli strain DH10B (Novagen), the resulting plasmid was isolated utilizing the Qiaprep Spin Mini-prep kit (Qiagen). Subsequently, the fragment was cleaved with NdeI and HindIII endonucleases and inserted into the pET-23a(+) expression vector (Novagen), previously digested with the same restriction enzymes. The complete pyrH nucleotide sequence was determined by automated DNA sequencing to corroborate se-quence identity, integrity and to check the absence of mutations in the cloned fragment.

Expression and purification of recombinant MtUMPK

The recombinant plasmid pET-23a(+)::pyrH was transformed into BL21(DE3) E. coli electrocompetent cells (Novagen), and cells carrying the recombinant vector were selected on Luria–Bertani (LB) agar plates containing 50 µg mL^{-1} ampicillin [27]. A single col-ony was used to inoculate 50 mL of Terrific Broth (TB) medium con-taining the same antibiotic and grown overnight at 37 °C. Aliquots of this culture (2.5 mL) were used to inoculate 250 mL of TB medium in 5 × 1 L flasks supplemented with ampicillin (50 µg mL^{-1}) and grown at 37 °C and 180 rpm to an optical density (OD$_{600nm}$) of 0.4–0.6. When this OD$_{600}$ value was reached, the temperature was low-ered to 30 °C and protein expression was carried out without isopro-pyl-β-D-thiogalactopyranoside (IPTG) induction. After 24 h, the cells (12 g) were collected by centrifugation at 11,800g for 30 min at 4 °C and stored at −20 °C. The same protocol was employed for BL21 (DE3) E. coli cell transformed with pET-23a(+) as control. The expres-sion of the recombinant protein was confirmed by 12% sodium

Fig. 1. Chemical reaction catalyzed by UMPK.

dodecyl sulfate–polyacrylamide gel electrophoresis (SDS–PAGE) stained with Coomassie Brilliant Blue [28].

Escherichia coli (2 g) cells overproducing the MtUMPK were resuspended in 20 mL of 50 mM Tris–HCl, pH 7.5 (buffer A), stirred for 30 min at 4 °C in the presence of lysozyme (0.2 mg mL^{-1}, Sigma–Aldrich), and disrupted by sonication (eight pulses of 10 s, at an amplitude value of 60%). The lysate was centrifuged at 38,900g for 30 min to remove cell debris and the supernatant was treated with 1% (wt/vol) streptomycin sulfate (Sigma–Aldrich), stirred for 30 min, and the mixture was centrifuged at 38,900g for 30 min. The supernatant containing soluble MtUMPK was dialyzed against 2 L of buffer A for 3 h.

All purification steps were carried out on an ÄKTA system (GE Healthcare) at 4 °C with UV detection at 215, 254, and 280 nm, and fractions were analyzed by SDS–PAGE. The crude extract was loaded on a HiPrep 16/10 Q XL (GE Healthcare) anion-exchange column pre-equilibrated with buffer A. Proteins were eluted using a 0–300 mM NaCl linear gradient at a flow rate of 1 mL min^{-1}. Fractions containing MtUMPK in NaCl (ca. 280 mM) were pooled and (NH$_4$)$_2$SO$_4$ was added to a final concentration of 1 M, stirred for 30 min, and clarified by centrifugation at 38,900g for 30 min. The supernatant was loaded on a Butyl Sepharose High Performance (GE Healthcare) hydrophobic interaction column pre-equilibrated with 50 mM Tris–HCl, pH 7.5, containing 1 M (NH$_4$)$_2$SO$_4$. Proteins were eluted using a 0–100% linear gradient of buffer A at a flow rate of 1 mL min^{-1}. Pooled fractions containing MtUMPK was dialyzed against buffer A to remove salt and loaded on a Mono Q 16/10 (GE Healthcare) anion-exchange column. MtUMPK was eluted in a salt gradient (0–240 mM NaCl) at a flow rate of 1 mL min^{-1}. The pooled sample was dialyzed against 50 mM Tris–HCl, pH 7.5, containing 200 mM NaCl, concentrated using an AMICON (Millipore Corporation, Bedford, MA) ultra filtration membrane (MWCO = 10 kDa), and stored at −80 °C. Total protein concentration was determined by the method of Bradford [29], using the Bio-Rad protein assay kit (Bio-Rad Laboratories) and bovine serum albumin as standard.

Amino acid sequence and mass spectrometry analysis

The N-terminal amino acid residues of homogenous recombinant MtUMPK were determined by automated Edman degradation sequencing using a PPSQ-21A gas-phase sequencer (Shimadzu) [30]. Recombinant MtUMPK was analyzed by electrospray ionization mass spectrometry (ESI-MS) employing some adaptations made to the system described by Chassaigne and Lobinski [31]. Samples were analyzed on a Quattro-II triple-quadrupole mass spectrometer (Micromass; Altrincham, UK), using MassLynx and Transform softwares for data acquisition and spectrum handling.

Determination of MtUMPK molecular mass

Gel-filtration chromatography was performed on a Superdex 200 (HR 10/30) column (GE Healthcare) pre-equilibrated with 50 mM Tris HCl pH 7.5 containing 200 mM NaCl at a flow rate of 0.4 mL min^{-1}, with UV detection at 215, 254 and 280 nm. The LMW and HMW Gel Filtration Calibration Kits (GE Healthcare) were used to prepare a calibration curve. The elution volumes (V_e) of standard proteins (ferritin, catalase, aldolase, coalbumin, ovalbumin, ribonuclease A) were used to calculate their corresponding partition coefficient (K_{av}, Eq. (1)). Blue dextran 2000 (GE Healthcare) was used to determine the void volume (V_o). V_t is the total bead volume of the column. The K_{av} value for each protein was plotted against their corresponding molecular mass.

$$K_{av} = \frac{V_e - V_o}{V_t - V_o} \tag{1}$$

Multiple sequence alignment

The amino acid sequences of the following UMPK proteins, whose three-dimensional structures were solved, were included in the alignment: E. coli (NP_414713.1), Ureaplasma parvum (YP_001752598.1), Pyrococcus furiosus (NP_579136.1), Sulfolobus solfataricus (NP_342460.1), and Bacillus anthracis (NC_012659.1). The UMPK amino acid sequences of S. pneumoniae (YP_816317.1) and B. subtilis (NP_389533.2) [32] were also included in the alignment and compared with M. tuberculosis UMPK (NP_217399.1). Multiple amino acid sequence alignment was performed by ClustalW [33], using the Gonnet matrix for amino acids substitutions and considering gap penalties, to identify essential residues for nucleotide substrate(s) binding, as well as to infer possible similarities in their mechanism of catalysis. For alignment improvement, 8, 23, 11, 5, 5, and 29 amino acids residues were removed from the E. coli, U. parvum, B. anthracis, S. pneumoniae, B. subtilis, and M. tuberculosis, respectively.

Functional characterization of MtUMPK

MtUMPK catalytic activity was measured for all purification steps in the forward direction at 25 °C, using a coupled spectrophotometric assay (0.5 mL final volume) as described elsewhere [34], on an UV-2550 UV/vis spectrophotometer (Shimadzu). In short, the reaction mixture contained 50 mM Tris–HCl, pH 7.5, 50 mM KCl, 5 mM MgCl$_2$ buffer; 1 mM phosphoenolpyruvate, 0.2 mM β-NADH, fixed concentrations of both ATP (3000 μM) and UMP (600 μM) substrates, 3 U of pyruvate kinase (EC 2.7.1.40) and 2.5 U of L-lactate dehydrogenase (EC 1.1.1.27). The reaction was started by the addition of MtUMPK. The decrease in absorbance at 340 nm ($\varepsilon_{\beta\text{-NADH}} = 6.22 \times 10^{+3}$ M^{-1} cm^{-1}) was continuously monitored and corrected for non-catalyzed chemical reactions in the absence of UMP. One unit of MtUMPK is defined as the amount of enzyme necessary to convert 1 μmol of UMP in UDP per min in an optical path of 1 cm.

Steady-state kinetics

Determination of the apparent steady-state kinetic parameters were evaluated at varying concentrations of UMP (0–150 μM) and a fixed-saturating concentration of ATP (3000 μM), and at varying concentrations of ATP (0–3000 μM) and a fixed-saturating level of UMP (600 μM). Initial velocity data were analyzed by SigmaPlot (Systat Software, Inc.).

In order to evaluate the specificity for phosphate acceptor, UMP was replaced with other nucleoside monophosphates (CMP, dCMP or dTMP) at different concentrations. The specificity of the enzyme as regards the phosphoryl donors was tested by replacing ATP with 3 mM GTP, CTP, and UTP in the standard assay.

Inhibition studies were carried out in the presence of fixed non-saturating levels of ATP (1300 μM) and fixed-varied UTP concentration (0, 30, 50, and 70 μM) when UMP was the variable substrate. Inhibition studies were also carried out in the presence of fixed non-saturating concentration of UMP (40 μM) and fixed-varied UTP concentration (0, 20, 50, and 100 μM) when ATP was the variable substrate. In addition, saturation curves for UTP (0–400 μM) were carried out at three different sets of experiments: fixed-non-saturating ATP concentration (1300 μM) corresponding to its $K_{0.5}$, and saturating UMP concentration (600 μM = 19 × K_m); fixed-non-saturating ATP concentration (1300 μM) corresponding to its $K_{0.5}$, and non-saturating UMP concentration (30 μM ≅ K_m); and fixed-saturating ATP concentration (3000 μM = 2.3 × $K_{0.5}$) and non-saturating UMP concentration (30 μM ≅ K_m). The maximal rate for each reaction condition was determined in the absence of inhibitor. Initial velocity parameters were also analyzed as a

function of ATP concentrations at fixed-saturating UMP concentration (600 μM) either in the absence or presence of a fixed concentration of GTP (500 μM) to verify whether this substrate has any effect on the kinetic properties of MtUMPK (70 nM). Initial velocity measurements were also carried out as a function of UMP concentration at fixed-saturating ATP concentration (3000 μM) in either absence or presence of GTP (500 μM).

Hyperbolic saturation curves were fitted by non-linear regression analysis to the Michaelis–Menten equation (Eq. (2)), in which v is the steady-state velocity, V_{max} is the maximal rate, $[S]$ is the substrate concentration, and K_m is the Michaelis–Menten constant [35,36]. Sigmoidal curves were fitted to the Hill equation (Eq. (3)), where $K_{0.5}$ is the value of the substrate concentration where $v = 0.5 V_{max}$, and n is the Hill coefficient (indicating the cooperative index) [35,36].

$$v = \frac{V_{max}[S]}{K_m + [S]} \tag{2}$$

$$v = \frac{V_{max}[S]^n}{K_{0.5}^n + [S]^n} \tag{3}$$

The K_i value for UTP towards UMP was calculated using the uncompetitive equation (Eq. (4)), in which $[I]$ is the inhibitor concentration and K_i is the inhibition constant [35,36].

$$v = \frac{V_{max}[S]}{[S]\left(1 + \frac{[I]}{K_i}\right) + K_m} \tag{4}$$

The IC_{50} value, which defines the concentration of inhibitor required to half-saturate the enzyme population, was determined by fitting the data to Eq. (5), in which v_i and v_o are, respectively, the reaction velocity in the presence and in the absence of inhibitor, v_i/v_o represents the fractional activity remaining at a given inhibitor concentration (fraction of free enzyme), and n is the Hill coefficient [36].

$$\frac{v_i}{v_o} = \frac{1}{1 + \left(\frac{[I]}{IC_{50}}\right)^n} \tag{5}$$

Isothermal titration calorimetry (ITC)

ITC experiments were carried out using an iTC$_{200}$ Microcalorimeter (MicroCal, Inc., Northampton, MA). The reference cell (200 μL) was loaded with Milli Q water during all experiments and the sample cell (200 μL) was filled with MtUMPK at a concentration of 100 μM. The injection syringe (39.7 μL) contained substrates or effectors at different concentrations: ATP, ADP, GTP, and UTP at 1.5 mM, UMP at 3 mM, and UDP at 1.8 mM. In addition, titration was performed with the non-hydrolyzable ATP analog, adenosine 5′-(β,γ-imido)triphosphate tetralithium salt hydrate (AMP-PNP) at 1.2 mM to determine the ligand concentration necessary to saturate the enzyme active sites. Subsequently, UMP at 800 μM was titrated into the sample cell containing MtUMPK (100 μM) and AMP-PNP at saturating concentration (250 μM). The latter permits evaluation of any effect that this ATP analog may have on UMP binding to MtUMPK:AMP-PNP binary complex. The ligand binding isotherms were measured by direct titration (ligand into macromolecule). The enzyme was prepared for ITC analysis by dialysis against 50 mM Hepes at pH 7.5 containing 50 mM KCl, 5 mM MgCl$_2$, 200 mM NaCl. The same buffer was used to prepare all ligand solutions and Tris, used at the kinetic assays, was replaced with Hepes due to the high enthalpy of ionization of Tris [37,38]. The stirring speed was 500 rpm at a temperature of 25 °C for all ITC experiments. The first titration injection (0.5 μL), which was discarded in the data analysis, was followed by 17 injections of 2.2 μL each at 180 s intervals. Control titrations (ligand into buffer)

were performed to subtract the heats of dilution and mixing for each experiment prior to data analysis. The data after peak integration of the isotherm generated by ITC, subtraction of control titration data and concentration normalization (heat normalized to the molar ratio), were analyzed by Origin 7 SR4 software (Microcal, Inc.).

The ΔG (Gibbs free energy) of binding was calculated using the relationship described in Eq. (6), in which R is the gas constant (8.314 J K^{-1} mol^{-1}), T is the temperature in K (T = °C + 273.15), and K_a is the association constant at equilibrium. The entropy of binding (ΔS) can also be determined by this mathematical formula. The initial estimates for n, K_a, and ΔH parameters were refined by standard Marquardt non-linear regression method provided in the Origin 7 SR4 software.

$$\Delta G^o = -RT \ln K_a = \Delta H^o - T\Delta S^o \tag{6}$$

Results and discussion

Amplification, cloning and sequencing of the pyrH gene

The 786-bp PCR amplicon was consistent with the M. tuberculosis H37Rv pyrH coding region (data not shown). The product was purified and ligated into pET-23a(+) expression vector as described in Section 'Amplification, cloning and DNA sequencing of the pyrH gene'. Automated DNA sequencing confirmed the identity and the absence of mutations in the cloned fragment.

Expression and purification of the recombinant MtUMPK

The resulting pET-23a(+)::pyrH recombinant plasmid was electroporated into BL21(DE3) E. coli cells and cultures were grown in TB medium for 24 h. Analysis by SDS–PAGE indicated that the supernatant of cell extract (Fig. 2A, lane 3), which was sonicated and centrifuged, contained a significant amount of protein with subunit molecular mass (ca. 27 kDa) in agreement with the predicted MW for MtUMPK (27.4 kDa).

The overexpressed protein was purified by a three-step protocol consisting of an anion-exchange column (HiPrep Q XL), a hydrophobic interaction column (Butyl Sepharose HP) and a strong anion-exchange column (Mono Q). The target protein eluted at approximately 180 mM of NaCl from the Mono Q column, and
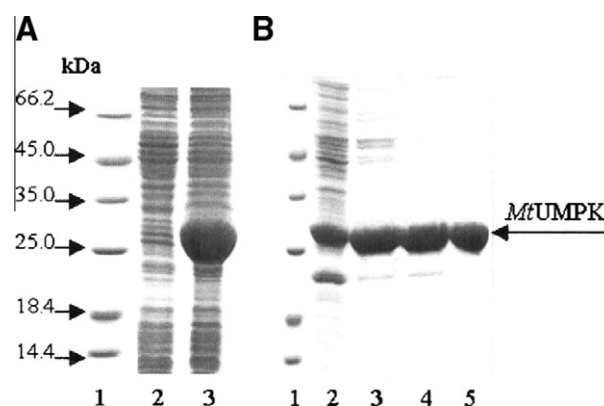
Fig. 2. (A) Twelve percent SDS–PAGE analysis of total soluble proteins. Expression of MtUMPK of 24-h cell growth after reaching an OD$_{600\,nm}$ of 0.4–0.6 in TB medium without addition of IPTG. Lane 1, Protein Molecular Weight Marker (Fermentas); lane 2, soluble E. coli BL21 (DE3) [pET-23a(+) (control)] extract; lane 3, soluble E. coli BL21 (DE3) [pET-23a(+)::pyrH] extract. (B) Twelve percent SDS–PAGE analysis of pooled fractions from MtUMPK purification steps. Lane 1, Protein Molecular Weight Marker (Fermentas); lane 2, crude extract; lane 3, HiPrep Q XL 16/10 elution; lane 4, Butyl Sepharose HP elution and Mono Q 16/10 elution.

Table 1
Purification of *Mt*UMPK from *E. coli* BL21 (DE3). Typical purification protocol from 2 g wet cell paste.

Purification step	Total protein (mg)	Total enzyme activity (U)	Specific activity (U mg^{-1})	Purification fold	Yield (%)
Crude extract	158	722	4.6	1.0	100
HiPrep Q XL	55	977	17.8	3.9	135
Butyl Sepharose	27	863	32	6.9	120
Mono Q	20	154	7.7	1.7	21

SDS–PAGE analysis showed that recombinant *Mt*UMPK was homogenous (Fig. 2B, lane 5). This 1.7-fold purification protocol yielded 20 mg of recombinant protein from 2 g of cells, indicating a 21% protein yield (Table 1). Enzyme kinetic measurements by NADH-coupled spectrophotometric assay showed that recombinant *Mt*UMPK indeed catalyzes the phosphorylation of UMP. Nevertheless, increase in the specific activity could be observed in the presence of high salt concentrations and a pronounced decrease after salt removal. This difference in activity may be attributed to ionic strength which, such as pH variations, is recognized to affect enzyme conformation, stability and activity [39,40]. Gagyi et al. [18] have also reported the addition of 100 mM NaCl as an approach to keep the *B. subtilis* UMPK stability. Accordingly, the homogenous protein was stored at −80 °C 50 mM Tris–HCl, pH 7.5, buffer containing 200 mM NaCl, which resulted in an apparent maximum velocity of 7.7 U mg^{-1} and allowed the kinetic assays to be carried out without affecting the coupled enzymes.

Mass spectrometry and N-terminal amino acid sequencing

The subunit molecular mass value was determined to be 27264.08 ± 13 Da by ESI-MS, which is lower than expected from the predicted amino acid sequence (27395.00 Da), indicating that the N-terminal methionine (130.92 Da) was removed.

The first 22 N-terminal amino acid residues identified by the Edman degradation method correspond to those predicted for the *pyrH* gene protein product and corroborate the N-terminal methionine removal. These results unambiguously identify the homogenous recombinant protein as the putative *Mt*UMPK.

MtUMPK molecular mass determination

The molecular mass of the native enzyme was determined by gel-filtration chromatography and yielded a single peak with elution volume corresponding to approximately 106 kDa, suggesting that *Mt*UMPK is a tetramer in solution (106,000 Da/27264.08 Da ≅ 3.9), differing from other bacterial homohexameric UMPKs [17–19].

Multiple sequence alignment

The currently available three-dimensional structures of UMPKs from several prokaryotic organisms deposited in the Protein Data Bank, such as *E. coli* (PDB code: 2BNE, 2BND, 2BNF, and 2V4Y) [13,41], *U. parvum* (PDB code: 2VA1) [21], *P. furiosus* (PDB code: 2BRI and 2BMU) [11], *S. solfataricus* (PDB code: 2J4J, 2J4K and 2J4L) [20] and *B. anthracis* (PDB code: 2JJX) [9], allow drug design based on a detailed model of the target binding site. The experimentally solved structures of *E. coli* UMPK [13,41] in complex with its substrates and the allosteric effector permit to propose the amino acid side chains in *M. tuberculosis* that are involved in ATP, UMP, and UDP binding as well as residues that participate in GTP-binding. To this end, multiple sequence alignment was carried out and
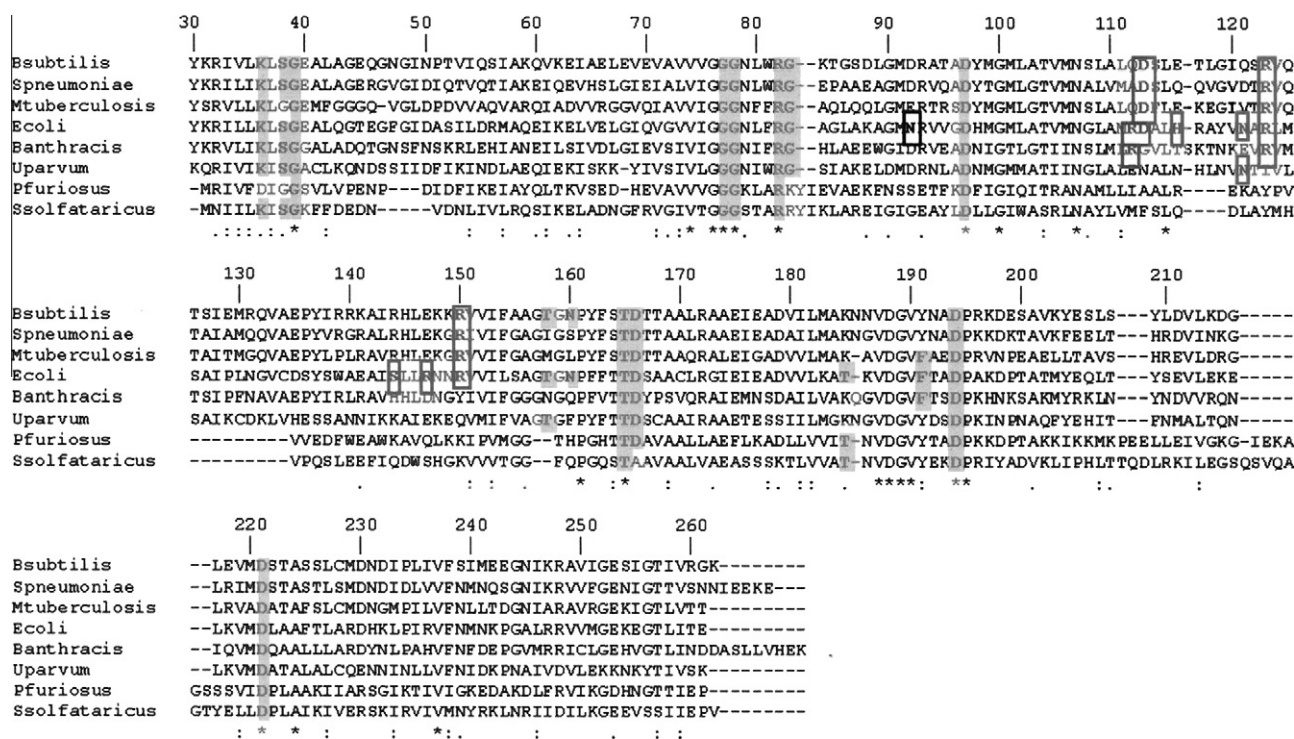
Fig. 3. Amino acids sequence alignment of UMPKs from eight prokaryotes. The residues inferred in *E. coli* as interacting with ATP, UMP or UDP are shaded in gray and the residues involved in GTP-binding are boxed [13,41]. (∗), (:), (.) and (−) indicate identity, strong similarity, weak similarity and gat inclusion among the residues, respectively. Amino acid residues were numbered after removing 29 N-terminal amino acids from the polypeptide sequence of *Mt*UMPK.

the results suggest that the conserved *Mt*UMPK Gly83 and Asp97 (*M. tuberculosis* numbering) amino acid residues are equivalent to residues in *E. coli* UMPK [13] that interact with the 2′-OH ribose ring of UMP (Fig. 3). The amino acids Gly77, Gly78, Arg82, and Thr165, which are involved in UMP α-phosphate interactions, are conserved among all sequences aligned. The main differences among UMP binding residues are those associated with uracil binding. The interactions between *E. coli* UMPK and the uracil moiety of UMP are between the hydrophilic Thr138 and Asn140 amino acids, whereas in *Mt*UMPK these interactions are made by the hydrophobic Met158 and Leu160 residues. As no structural data for *Mt*UMPK have been available to date, it is tempting to suggest that these differences may be related to the distinct quaternary structures of *Mt*UMPK (tetramer) and *E. coli* UMPK (hexamer), since site-directed mutagenesis of Thr138 and Asn140 residues suggested their involvement in subunit contacts in the quaternary structure of the latter [13]. The interactions between the enzyme and uracil, ribose, or the UDP α-phosphate moiety are very similar to those with UMP, although UDP binding involves three additional amino acid residues [13]. The Lys36 and Gly39 residues (*M. tuberculosis* numbering) are conserved, whereas Gly39 in *Mt*UMPK sequence replaces a serine residue present in *E. coli* UMPK.

The amino acids Lys36, Asp166, Phe191, Asp194, and Asp221 in *Mt*UMPK are likely involved in ATP interaction since they are conserved in the *E. coli* UMPK and *Mt*UMPK polypeptide sequences. On the other hand, Lys185 in *Mt*UMPK replaces a threonine residue present in ATP binding site of *E. coli* UMPK. It is interesting to note that the Lys residue involved in ATP binding replaces Thr in five UMPK sequences [43] as in *Mt*UMPK. In *E. coli* UMPK, the GTP-binding site is between two dimers of the hexamer and GTP promotes a rearrangement of its quaternary structure, resulting in a tighter dimer–dimer interaction [41]. Asp113, which interacts with the GTP purine moiety, Arg123 and Arg150, both interacting with the phosphate group, are the most conserved amino acid residues (Fig. 3). These residues are absent in *U. parvum* and *S. solfataricus* UMPKs and may explain the lack of GTP stimulation of these enzymes [20,21].

*Mt*UMPK kinetic parameters

The dependence of velocity with UMP as variable substrate at fixed-saturating ATP concentration (3000 μM) followed hyperbolic Michaelis–Menten kinetics (Fig. 4A), and the apparent constant values were thus calculated fitting the data to Eq. (2), yielding the following values: V_{max} = 7.5 (±0.3) U mg^{-1} and K_m = 31 (±3) μM. These results permit estimate a value of 3.4 (±0.1) s^{-1} for the UMP catalytic constant (k_{cat}) and of 11 (±1) × 10^4 M^{-1}s^{-1} for the UMP specificity constant (k_{cat}/K_m). The Michaelis–Menten constant values are similar to those reported for *B. subtilis* (K_m^{UMP} = 30 μM) and *E. coli* (K_m^{UMP} = 43 μM at pH 7.4) UMPKs [18,41].

The saturation curve for ATP at fixed-saturating UMP concentration (600 μM) was sigmoidal (Fig. 4B), suggesting cooperative kinetics. Accordingly, the data were fitted to the Hill equation (Eq. (3)), yielding the following values: V_{max} = 8.8 (±0.2) U mg^{-1}, $K_{0.5}$ = 1299 (±32) μM and n = 3.9 (±0.3). The k_{cat} for ATP is 4.0 (±0.1) s^{-1}. The limiting value for the Hill coefficient (n) is four since we showed that *Mt*UMPK is a homotetramer in solution. The n value of 3.9 thus indicates strong positive cooperativity for ATP.

As demonstrated for others UMPKs [17,20,21], *Mt*UMPK was specific for UMP as the phosphoryl group acceptor as no enzyme activity was detected with CMP, dCMP or dTMP. The specificity for the phosphoryl group donor was tested with GTP, CTP and UTP, and UMP as the acceptor substrate. No activity was detected with GTP and CTP. UTP acted as phosphoryl donor at a velocity value of 0.5 U mg^{-1}. This value is 18-fold lower than for ATP
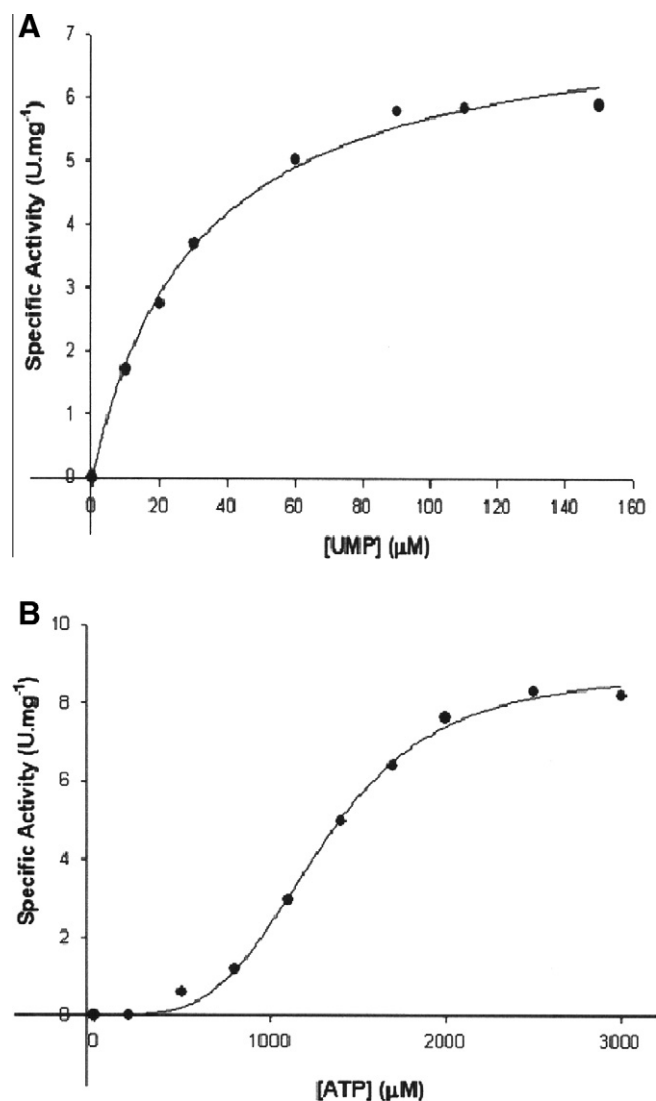

Fig. 4. Apparent steady-state kinetic parameters. (A) Specific activity (U mg^{-1}) versus [UMP] (μM) at fixed concentration of ATP (3000 μM). (B) Specific activity (U mg^{-1}) versus [ATP] (μM) at fixed concentration of UMP (600 μM). The *Mt*UMPK concentration was 70 nM on both assays.

(8.8 U mg^{-1}), suggesting that ATP is the more likely physiological phosphate donor for *Mt*UMPK.

UTP has been reported as a common negative regulator of UMP-Ks from Gram-negative bacteria, Gram-positive bacteria and archae [20,42,43]. To evaluate the inhibitory effect of UTP on *Mt*UMPK enzyme velocity, measurements of steady-state rates were carried out as described in Section 'Materials and methods'. Double-reciprocal plots at different UTP concentrations displayed a pattern of parallel lines, suggesting that UTP acts as an uncompetitive inhibitor towards UMP in which V_{max} and K_m values were simultaneously reduced (Fig. 5) at fixed non-saturating ATP concentration (1300 μM) and varying UMP concentration. Data fitting to Eq. (4) for uncompetitive inhibition yielded a K_i value of 87 (±5) μM for UTP. On the other hand, the plots of *Mt*UMPK activity versus ATP concentration in the presence of both non-saturating UMP (40 μM) and fixed-varied UTP concentrations (0, 30, 50, and 70 μM) were all sigmoidal. Although inhibition by UTP did not modify the sigmoidal shape of the curve, data fitting to Eq. (3) yielded increasing, though modest, values for apparent $K_{0.5}$, whereas V_{max} and the Hill coefficient values remained approximately constant (Table 2). These features appear to be a common
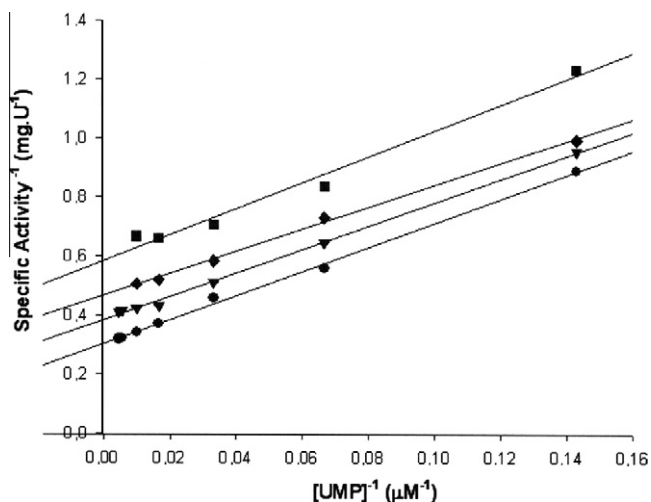
Fig. 5. Double-reciprocal plot of specific activity^{-1} (mg U^{-1}) versus [UMP]$^{-1}$ (μM^{-1}) at 0, 30, 50 and 70 μM UTP. The *Mt*UMPK concentration was 80 nM.

theme for UMPKs from Gram-positive and archae microorganisms [19,20,43].

The saturation curves for UTP inhibition in the presence of fixed-non-saturating ATP concentration and saturating UMP concentration, fixed-non-saturating ATP concentration and non-saturating UMP concentration, and fixed-saturating ATP concentration and non-saturating UMP concentration were all sigmoidal (data not shown). These data were thus fitted to Eq. (5), yielding estimates for IC_{50} values and the Hill coefficient (Table 3). The rates decreased with increasing UTP concentration, reaching a plateau of low enzyme activity (below 0.5 U mg^{-1}) at high UTP concentrations. The IC_{50} values of 80 μM (saturating UMP concentration) and 97 μM (non-saturating UMP concentration) were within experimental error. These results are in agreement with UTP acting as an uncompetitive inhibitor towards UMP (Fig. 5), thereby suggesting that UTP preferentially binds to a complex formed between *Mt*UMPK and UMP (it would have to be a ternary complex because we showed that ATP binding is followed by UMP binding). Stated otherwise, as the *Mt*UMPK enzyme mechanism is ordered (ATP binds first), the concentration of *Mt*UMPK:ATP binary complex, to which UMP binds, is unchanged as ATP concentration in both experiments were the same (1300 μM). It could be argued that

increasing UMP fixed concentration (from 30 to 600 μM) would result in increasing concentration of *Mt*UMPK:ATP:UMP ternary complex, to which UTP binds, resulting in lower IC_{50} values for larger UMP concentrations. However, it should be kept in mind that the enzyme activity measurements here presented provide a value for the apparent K_m value of UMP and that this value represents an apparent dissociation constant that may be treated as the overall dissociation constant of all enzyme-bound species. In short, the true equilibrium dissociation constant of UMP from *Mt*UMPK: ATP:UMP ternary complex is not known, thereby precluding a proposal that increasing UMP concentration would result in increasing ternary complex concentration because the true dissociation constant value for UMP may be considerably larger than the concentrations employed here. In any case, the uncompetitive inhibition cannot be overcome by high UMP substrate concentrations, suggesting that UTP binds to an allosteric (regulatory) site. In addition, there was a decrease in the Hill coefficient (n) from 2.8 at non-saturating UMP concentration to 1.5 at saturating UMP concentration (Table 3). It thus appears that increasing UMP concentration results in decreasing degree of cooperativity. In the presence of saturating ATP concentration (3000 μM), there was a 2-fold increase in IC_{50} value for UTP, suggesting that UTP acts as a competitive inhibitor towards ATP. These data are consistent with ATP kinetics in which increasing fixed-varied concentrations of UTP in the presence of fixed-non-saturating UMP concentration yielded increasing values for apparent $K_{0.5}$ (Table 2). Moreover, since we have shown that UTP can act as a poor phosphoryl donor, it is thus likely that UTP can also bind to ATP binding site of *Mt*UMPK. These data suggest that UTP either binds to the ATP binding site with low affinity or to an allosteric site that results in uncompetitive inhibition towards UMP. Incidentally, it has been proposed that each subunit of bacterial UMPKs has three distinct nucleotide-binding sites [43].

GTP has been shown to be a positive effector for bacterial UMP-Ks [41,43]. The crystal structure of *E. coli* UMPK bound to GTP has recently been solved at 2.3 Å [41]. The presence of GTP (500 μM) resulted in both increased V_{max} values (from 2 to 3.2 U mg^{-1}) and affinity ($K_{0.5}$) of ATP for *Mt*UMPK (from 1335 to 545 μM) (Fig. 6). In addition, the Hill coefficient value of 4.4 in the absence of GTP decreased to 1.6 in the presence of GTP (500 μM), suggesting that this nucleotide decreased the degree of cooperativity of ATP upon *Mt*UMPK enzyme activity (Fig. 6). These results are in agreement with previously published results on UMPKs from Gram-positive bacteria [19,43]. On the other hand, the effect of GTP on UMP kinetics displayed a slight increase in the V_{max} values (from 1.63 ± 0.03 U mg^{-1} in the absence to 2.07 ± 0.05 U mg^{-1} in the presence of GTP), and no change of K_m values for UMP (data not shown).

Equilibrium binding of ligands assessed by ITC

To further elucidate the *Mt*UMPK kinetic mechanism, titration microcalorimetry of ligand binding to the recombinant enzyme was carried out. Equilibrium binding values of ligands were measured directly by ITC, determining the heat generated or consumed upon ligand–macromolecule binary complex formation at constant temperature and pressure. The measured of the heat released upon binding of the ligands allowed us to derive the binding enthalpy (ΔH) of the process, to estimate the stoichiometry of the interaction (n) and the association constant at equilibrium (K_a). The dissociation constant at equilibrium (K_d) could be calculated as the inverse of K_a ($K_d = 1/K_a$). Moreover, the Gibbs free energy (ΔG) and entropy (ΔS) of binding were determined from the association constant values at equilibrium as described in Eq. (6). The ITC data for binding of ligands to *Mt*UMPK (Fig. 7) are summarized in Table 4. The overall binding isotherms for ATP, ADP, UDP or

Table 2
ATP kinetic parameters in the presence of fixed concentrations of UTP.

UTP concentration (μM)	V_{max}[a]	n[b]	$K_{0.5}$[c] (μM)
0	3.8 ± 0.3	2.4 ± 0.4	1.2 (±0.1) × 10^3
20	3.5 ± 0.3	2.1 ± 0.3	1.3 (±0.2) × 10^3
50	3.9 ± 0.4	2.5 ± 0.5	1.4 (±0.2) × 10^3
100	4 ± 1	2.3 ± 0.9	1.7 (±0.5) × 10^3

[a] V_{max} = maximal rate.
[b] n = the Hill coefficient.
[c] $K_{0.5}$ = value of the substrate concentration in which $v = 0.5\,V_{max}$.

Table 3
IC_{50} and n values for UTP in the presence of different fixed substrate concentrations.

Substrate concentrations	IC_{50}[a] (μM)	n[b]
ATP 1300 μM + UMP 600 μM	80 ± 4	1.5 ± 0.1
ATP 1300 μM + UMP 30 μM	97 ± 7	2.8 ± 0.4
ATP 3000 μM + UMP 30 μM	210 ± 6	3.6 ± 0.3

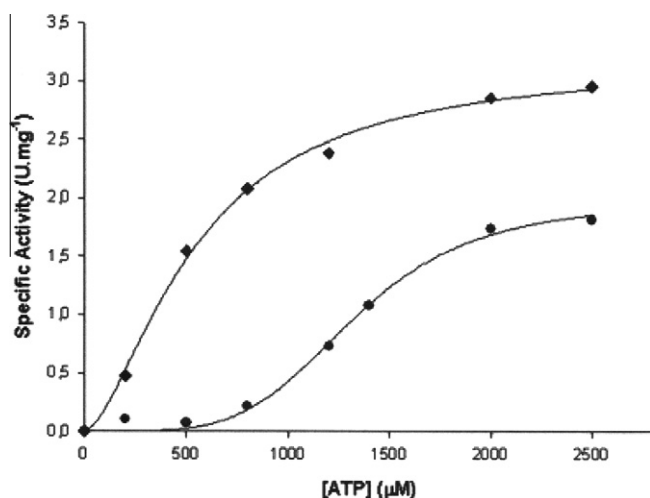[a] IC_{50} = concentration of inhibitor required to half-saturate the enzyme population.
[b] n = the Hill coefficient.

Fig. 6. Effect of GTP (500 μM) on ATP saturation curves. In the absence of effector (●), the curve is sigmoidal. In the presence of effector (♦), the sigmoidicity is reduced though still present. The *Mt*UMPK concentration was 70 nM.

GTP-binding to *Mt*UMPK were best fitted to a model of one set of sites (Table 4). The UTP binding isotherm was not well defined to obtain an adequate fit of the data to any model, probable because this substrate may exert different and simultaneous effects on *Mt*UMPK.

The mechanism of phosphoryl transfer of NMP kinases has been reported to follow a sequential random bi bi kinetic mechanism [12]. The *Mt*UMPK appears to deviate from this type of mechanism, since no significant heat changes were obtained for UMP binding, suggesting that it cannot bind to free enzyme. In contrast, all other ligands tested do bind to the free enzyme and exhibit exothermic reactions, as seen by negative changes in the binding enthalpy (Fig. 7). Interestingly, the binding isotherm of an ATP molecule does not appear to influence the affinity for the subsequent one, as the thermodynamic parameters for ATP binding provide single ΔH and K_a values. How can one reconcile these data with positive cooperativity displayed by the saturation curve (Fig. 4B) of steady-state kinetics for ATP in the presence of UMP? These data suggest that ATP binding has a positive heterotropic effect upon UMP binding to *Mt*UMPK:ATP binary complex, since UMP does not bind to the free enzyme. The *n* value of 0.57 sites for the ATP binding refers to the event of two subunits of *Mt*UMPK in the cell associating with each ATP molecule injected. In summary, we propose that ATP binding triggers a conformational change of *Mt*UMPK that results in increased affinity for UMP. To provide further experimental evidence for the proposed positive heterotropic effect of ATP, titration of UMP into a solution containing *Mt*UMPK:AMP-PNP binary complex (a non-hydrolyzable ATP analog) was carried out. The ligand binding isotherms showed no ITC signal upon UMP binding to free *Mt*UMPK enzyme (Fig. 7, panel E). On the other hand, the ITC signal for titration of *Mt*UMPK:AMP-PNP with UMP showed changes in the degree of heat response upon *Mt*UMPK:AMP-PNP:UMP ternary complex formation, displaying exothermic and endothermic responses (Fig. 7, panel F). The ITC data were analyzed with a model assuming a cooperative ligand binding interaction for a tetrameric protein. The UMP binding exhibited biphasic behavior (Fig. 7, panel F), which could be assessed by the endothermic and exothermic profile of the heat response. The ITC data showed a cooperative pattern and demonstrated that UMP binds to *Mt*UMPK:AMP-PNP binary complex (Table 4), even though it could not be demonstrated an obvious positive cooperative effect with increasing affinity for UMP as the binding sites are sequentially occupied. However, positive cooperativity is generally more difficult to

distinguish from ITC studies alone, since the tendency is for the binding sites on any single molecule to saturate together unless the difference in affinity values between the sites were large. Notwithstanding, the ITC data are in agreement with the steady-state kinetics results showing that UMP binds to *Mt*UMPK:ATP binary complex and that ATP has a cooperative effect on tetrameric *Mt*UMPK enzyme.

The UDP product binds to free *Mt*UMPK enzyme with higher affinity than ADP product (Table 4), and both ligands displayed a stoichiometry of one ligand binding to each monomer of the tetrameric enzyme. The larger association constant of UDP as compared to ADP appears to be enthalpy driven (Table 4). These ITC results suggest that product release is random. The GTP-binding affinity is in the same range of UDP (Table 4). These ITC results demonstrate that GTP is capable of binding to free *Mt*UMPK enzyme with a stoichiometry close to unity. It is interesting to note that ATP (substrate) as compared to ADP (product) binding display approximately the same association constant at equilibrium (or Gibbs free energy), which is a result of the ubiquitous phenomenon of enthalpy–entropy compensation meaning that entropy losses often negate enthalpy gains [8]. In short, ITC and steady-state kinetic results provide evidence *Mt*UMPK follows an sequential ordered mechanism, in which ATP binds first to free enzyme followed by UMP binding to the *Mt*UMPK:ATP binary complex (Fig. 8). Release of products is, however, random. The mechanism for *S. solfataricus* UMPK has been shown to be random order for either addition of substrates or release of products [20].

Summary

Bacterial UMPKs have been proposed to be attractive drug targets because their primary amino acid sequence and three-dimensional structures are divergent from their eukaryotic counterparts. They are unique members of the NMP kinases family of enzymes and several research groups have demonstrate its essentiality for different organisms [17,19,25,26,44], and to *M. tuberculosis* in particular [24]. Moreover, they are oligomers with an exclusive and complex control of activity by GTP and UTP, representing an interesting model of allosteric regulation [43]. The elucidation of the mode of action of *Mt*UMPK is thus warranted. Although the *pyrH* gene has been proposed by *in silico* analysis to encode a UMPK enzyme [23], formal biochemical proof was still lacking as regards the correct assignment to its open reading frame in *M. tuberculosis*. Accordingly, here we describe PCR amplification of the *pyrH* coding region, cloning, heterologous expression, and purification of recombinant protein to homogeneity. N-terminal amino acid sequence and ESI-MS confirmed the identity of the homogeneous recombinant protein. Steady-state kinetic measurements confirmed that the *pyrH* gene encodes a UMPK enzyme in *M. tuberculosis*. Size exclusion chromatography showed that *Mt*UMPK is a tetramer in solution. Multiple sequence alignment analysis allowed identification of residues involved in substrate binding and/or catalysis.

Steady-state kinetic measurements showed that *Mt*UMPK is specific for both ATP and UMP substrates. This specificity for UMP is not surprising since it has been shown that the Rv1712 locus in *M. tuberculosis* codes for a functional cytosine monophosphate kinase that preferentially phosphorylates CMP and dCMP, and that UMP is a poor substrate [45]. In agreement with these results, *E. coli* has two distinct enzymes that display substrate specificity for UMP (UMPK) or CMP (CMP kinase) [46]. Steady-state kinetics and ITC data suggest a sequential ordered mechanism for substrate addition to *Mt*UMPK, in which ATP binds first to free enzyme followed by UMP binding; and a random order for release of products.
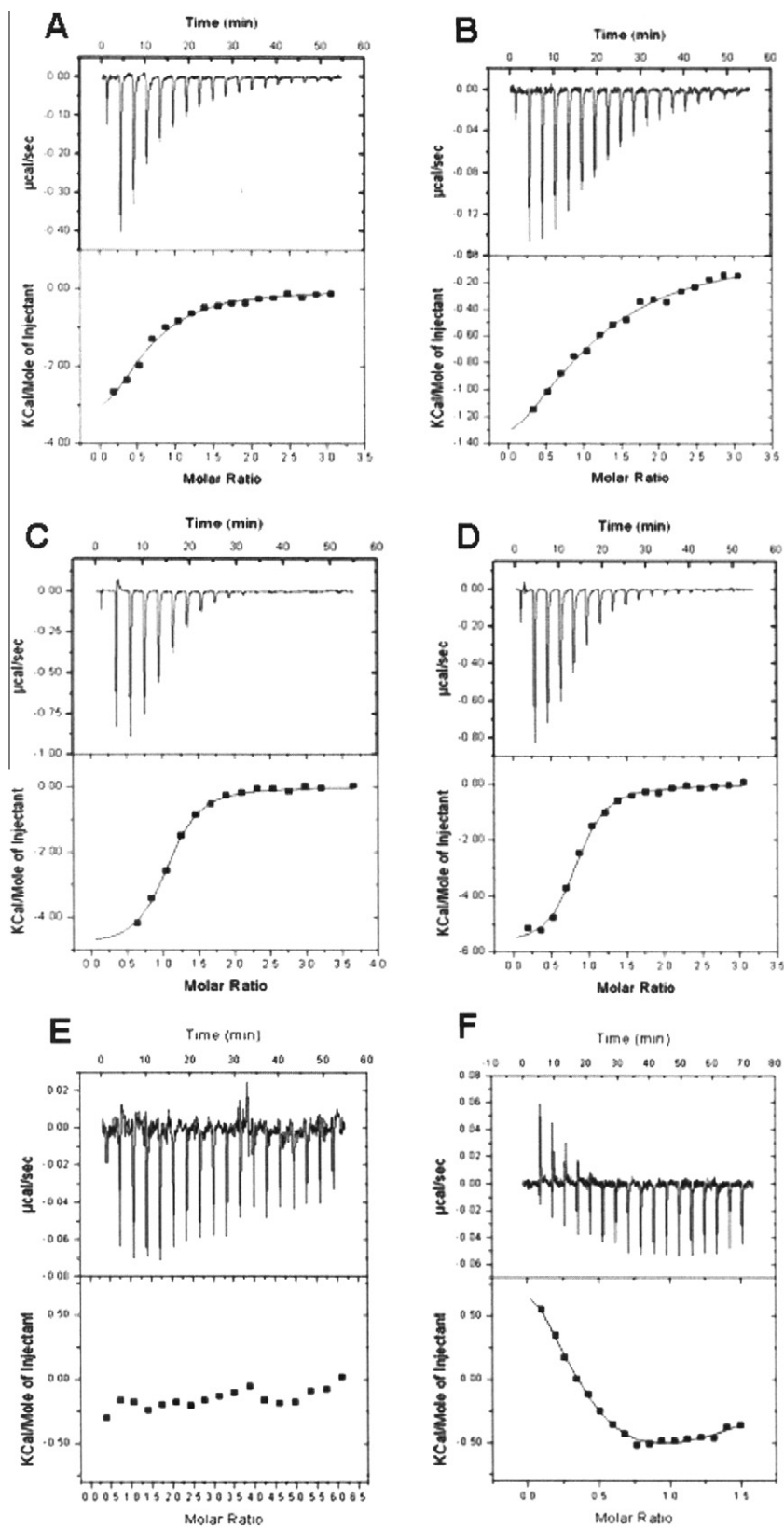
Fig. 7. Isothermal titration calorimetric curves of binding of ligands to *Mt*UMPK (100 μM). (A) Titration of the ATP substrate at a final concentration of 248 μM. (B) Titration of the ADP product at a final concentration of 248 μM. (C) Titration of the UDP product at a final concentration of 398 μM. (D) Titration of the allosteric effector GTP at a final concentration of 248 μM. (E) Titration of the UMP substrate at a final concentration of 497 μM. (F) Titration of the UMP substrate at a final concentration of 132 μM in the presence of the non-hydrolyzable ATP analog (AMP-PNP). The experiments were carried out at constant temperature and pressure.

Table 4
Association constants and thermodynamic parameters of different ligands binding to MtUMPK.

Ligands	n^a	K_a^b (M^{-1})	$\Delta H^{\circ c}$ (kcal mol^{-1})	$\Delta G^{\circ d}$ (kcal mol^{-1})	$\Delta S^{\circ e}$ (cal mol^{-1} K^{-1})	K_d^f (µM)
ATP	0.57 ± 0.06	3.0e^4 ± 5.7e^3	−4.8 ± 0.6	−6.1 ± 1.2	4.3 ± 0.8	33.3 ± 6.3
ADP	1.0 ± 0.1	1.5e^4 ± 3.5e^3	−2.1 ± 0.4	−5.7 ± 1.3	12.1 ± 2.8	66 ± 15
UDP	1.01 ± 0.01	2.1e^5 ± 2.4e^4	−4.9 ± 0.1	−7.3 ± 0.8	7.9 ± 0.9	4.8 ± 0.5
GTP	0.80 ± 0.01	2.0e^5 ± 2.6e^4	−5.8 ± 0.1	−7.2 ± 0.9	4.6 ± 0.6	5.0 ± 0.6
UMP		2.4e^5 ± 1.5e^5	0.68	−7.34	26.9	4.2 ± 2.6
		7.5e^4 ± 3.8e^4	−2.3	−6.63	14.6	13.3 ± 6.8
		1.5e^5 ± 9.3e^4	−3.0	−7.03	13.4	6.7 ± 4.2
		1.0e^5 ± 5.3e^4	7.9	−6.84	49.5	10 ± 5.3

[a] n = number of sites.
[b] K_a = association constant.
[c] ΔH° = binding enthalpy.
[d] ΔG° = Gibbs free energy.
[e] ΔS° = binding entropy.
[f] K_d = dissociation constant.
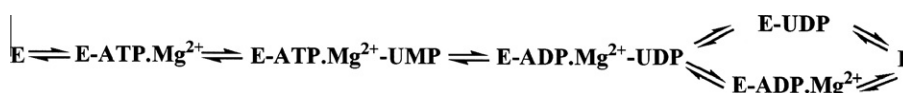
Fig. 8. Proposed kinetic mechanism for MtUMPK.

The cooperative kinetics with respect to ATP, activation by GTP, and inhibition by UTP, showed that MtUMPK is an allosteric enzyme that is subject to a complex control by these metabolites. The results here described also show that MtUMPK belongs to the K system. This term was originally proposed by Monod et al. [47], in which the enzyme exists at equilibrium between two states with the same catalytic activities, but different substrate affinities (T of low affinity, and R of high affinity). In the absence of effectors, ATP has a positive heterotropic effect on UMP binding to MtUMPK to form the catalytically competent ternary complex. This degree of cooperativity is decreased in the presence of GTP as there is a lowering of the Hill coefficient value, and a decrease in $K_{0.5}$ value for ATP, thereby suggesting increased ATP affinity for MtUMPK. This model may also be applicable to UTP inhibition, in which binding of UTP displaces the equilibrium for the state with lower affinity for ATP with no effect on the Hill coefficient and maximum velocity. Moreover, as UTP is an uncompetitive inhibitor towards UMP, it appears that UTP can have a dual inhibitory effect on MtUMPK enzyme activity depending on which substrate is varied. The results on MtUMPK mode of action show that its cooperativity is more pronounced than that observed for other UMPKs (n values of 1.28–2.5) [19,21,43]. In general, the Hill coefficient does not represent the actual number of sites, unless the cooperativity is high [35]. Our findings show that the n value of ATP (3.9) for tetrameric MtUMPK indicates strong positive cooperativity and it may correspond to the actual number of protomers. Activation of MtUMPK by GTP and feedback inhibition by UTP imply a role for this enzyme in coordinating the synthesis of purine versus pyrimidine nucleoside triphosphates, and highlights the likely relevance of UMP in the metabolism of M. tuberculosis.

The currently available repertoire of antimycobacterial agents reveals only a handful of comprehensively validated targets, namely RNA polymerase, DNA gyrase, NADH-dependent enoyl-ACP reductase, and ATP synthase [48]. The complete genome sequencing of M. tuberculosis H37Rv strain has accelerated the study and validation of molecular targets aiming at the rational design of anti-TB drugs [23]. The target-based rational design of new agents with anti-TB activity includes functional and structural efforts. However, the first step to enzyme target validation must include experimental data demonstrating that a gene predicted by in silico analysis to encode a particular protein catalyzes the proposed chemical reaction. Moreover, it has recently been pointed out that

recognition of the limitations of high-throughput screening approaches in the discovery of candidate drugs has rekindled interest in rational design methods [8]. Understanding the mode of action of MtUMPK will inform us on how to better design inhibitors targeting this enzyme with potential therapeutic application in TB chemotherapy. Accordingly, it is hoped that the results here described may be useful to the rational design of anti-TB agents and that they may contribute to our understanding of the biology of M. tuberculosis.

References

[1] C. Dye, S. Scheele, P. Dolin, V. Pathania, M.C. Raviglione, J. Am. Med. Assoc. 282 (1999) 677–686.
[2] World Health Organization, Global Tuberculosis Control: A Short Update to the 2009 Report, 2010.
[3] W.W. Yew, C.C. Leung, Respirology 13 (2008) 21–46.
[4] A.A. Velayati, P. Farnia, M.R. Masjedi, T.A. Ibrahim, P. Tabarsi, R.Z. Haroun, H.O. Kuan, J. Ghanavi, P. Farnia, M. Varahram, Eur. Respir. J. 34 (2009) 1202–1203.
[5] R.G. Ducati, L.A. Basso, D.S. Santos, Curr. Drug Targets 8 (2007) 423–435.
[6] J.G. Robertson, Biochemistry 44 (2005) 5561–5571.
[7] J.G. Robertson, Curr. Opin. Struct. Biol. 17 (2007) 674–679.
[8] J.E. Ladbury, G.K. Klebe, E. Freire, Nat. Rev. Drug Discov. 9 (2010) 23–27.
[9] C. Meier, L.G. Carter, S. Sainsbury, E.J. Mancini, R.J. Owens, D.I. Stuart, R.M. Esnouf, J. Mol. Biol. 381 (2008) 1098–1105.
[10] G.E. Shambaugh, Am. J. Clin. Nutr. 32 (1979) 1290–1297.
[11] C. Marco-Marín, F. Gil-Ortiz, V. Rubio, J. Mol. Biol. 352 (2005) 438–454.
[12] H. Yan, M.D. Tsai, Adv. Enzymol. Relat. Areas Mol. Biol. 73 (1999) 103–134.
[13] P. Briozzo, C. Evrin, P. Meyer, L. Assairi, N. Joly, O. Barzu, A. Gilles, J. Biol. Chem. 280 (2005) 25533–25540.
[14] H.J. Müller-Dieckmann, G.E. Schulz, J. Mol. Biol. 236 (1994) 361–367.
[15] J. Liou, G.E. Dutschman, W. Lam, Z. Jiang, Y. Cheng, Cancer Res. 62 (2002) 1624–1631.
[16] K. Scheffzek, W. Kliche, L. Wiesmüller, J. Reinstein, Biochemistry 35 (1996) 9716–9727.
[17] L. Serina, C. Blondin, E. Krin, O. Sismeiro, A. Danchin, H. Sakamoto, A.M. Gilles, O. Bârzu, Biochemistry 34 (1995) 5066–5074.
[18] C. Gagyi, N. Bucurenci, O. Sîrbu, G. Labesse, M. Ionescu, A. Ofiteru, L. Assairi, S. Landais, A. Danchin, O. Bârzu, A. Gilles, Eur. J. Biochem. 270 (2003) 3196–3204.
[19] F. Fassy, O. Krebs, M. Lowinski, P. Ferrari, J. Winter, V. Collard-Dutilleul, Biochem. J. 384 (2004) 619–627.
[20] K.S. Jensen, E. Johansson, K.F. Jensen, Biochemistry 46 (2007) 2745–2757.
[21] L. Egeblad-Welin, M. Welin, L. Wang, S. Eriksson, FEBS J. 274 (2007) 6403–6414.
[22] K.A. Kantardjieff, C. Vasquez, P. Castro, N.M. Warfel, B.S. Rho, T. Lekin, C.Y. Kim, B.W. Segelke, T.C. Terwilliger, B. Rupp, Acta Crystallogr. D: Biol. Crystallogr. 61 (2005) 355–364.
[23] S.T. Cole, R. Brosch, J. Parkhill, T. Garnier, C. Churcher, D. Harris, S.V. Gordon, K. Eiglmeier, S. Gas, C.E. Barry, F. Tekaia, K. Badcock, D. Basham, D. Brown, T. Chillingworth, R. Connor, R. Davies, K. Devlin, T. Feltwell, S. Gentles, N. Hamlin, S. Holroyd, T. Hornsby, K. Jagels, A. Krogh, J. McLean, S. Moule, L. Murphy, K.

Oliver, J. Osborne, M.A. Quail, M.A. Rajandream, J. Rogers, S. Rutter, K. Seeger, J. Skelton, R. Squares, S. Squares, J.E. Sulston, K. Taylor, S. Whitehead, B.G. Barrell, Nature 393 (1998) 537–544.

[24] D. Robertson, P. Carroll, T. Parish, Tuberculosis 87 (2007) 450–458.

[25] K. Yamanaka, T. Ogura, H. Niki, S. Hiraga, J. Bacteriol. 174 (1992) 7517–7526.

[26] J.C. Smallshaw, R.A. Kelln, Genetics (Life Sci. Adv.) 11 (1992) 59–65.

[27] J. Sambrook, D.W. Russel, Molecular Cloning: A Laboratory Manual, Spring Harbor Laboratory Press, New York, 2001.

[28] U.K. Laemmli, Nature 227 (1970) 680–685.

[29] M.M. Bradford, Anal. Biochem. 72 (1976) 248–254.

[30] B. Monson de Souza, M.S. Palma, Biochim. Biophys. Acta 1778 (2008) 2797–2805.

[31] H. Chassaigne, R. Lobinski, Analyst 123 (1998) 2125–2130.

[32] D.A. Benson, I. Karsch-Mizrachi, D.J. Lipman, J. Ostell, E.W. Sayers, Nucleic Acids Res. 37 (2009) D26–D31.

[33] J.D. Thompson, D.G. Higgins, T.J. Gibson, Nucleic Acids Res. 22 (1994) 4673–4680.

[34] J.S. Oliveira, C.A. Pinto, L.A. Basso, D.S. Santos, Protein Expr. Purif. 22 (2001) 430–435.

[35] I. Segel, Enzyme Kinetics, Behavior and Analysis of Rapid Equilibrium and Steady-State Enzyme Systems, John Wiley and Sons, New York, 1975.

[36] R.A. Copeland, Evaluation of Enzyme Inhibitors in Drug Discovery, John Wiley and Sons, Inc., New Jersey, 2005.

[37] R.G. Bates, H.B. Hetzer, J. Phys. Chem. 65 (1961) 667–671.

[38] H. Fukada, K. Takahashi, Proteins 33 (1998) 159–166.

[39] M.C. Pinna, A. Salis, M. Monduzzi, B.W. Ninham, J. Phys. Chem. B 109 (2005) 5406–5408.

[40] Y. Zhang, P.S. Cremer, Curr. Opin. Chem. Biol. 10 (2006) 658–663.

[41] P. Meyer, C. Evrin, P. Briozzo, N. Joly, O. Bârzu, A. Gilles, J. Biol. Chem. 283 (2008) 36011–36018.

[42] L. Serina, N. Bucurenci, A.M. Gilles, W.K. Surewicz, H. Fabian, H.H. Mantsch, M. Takahashi, I. Petrescu, G. Batelier, O. Bârzu, Biochemistry 35 (1996) 7003–7011.

[43] C. Evrin, M. Straut, N. Slavova-Azmanova, N. Bucurenci, A. Onu, L. Assairi, M. Ionescu, N. Palibroda, O. Bârzu, A. Gilles, J. Biol. Chem. 282 (2007) 7242–7253.

[44] S.E. Lee, S.Y. Kim, C.M. Kim, M. Kim, Y.R. Kim, K. Jeong, H. Ryu, Y.S. Lee, S.S. Chung, H.E. Choy, J.H. Rhee, Infect. Immun. 75 (2007) 2795–2801.

[45] C. Thum, C.Z. Schneider, M.S. Palma, D.S. Santos, L.A. Basso, J. Bacteriol. 191 (2009) 2884–2887.

[46] N. Bucurenci, H. Sakamoto, P. Briozzo, N. Palibroda, L. Serina, R.S. Sarfati, G. Labesse, G. Briand, A. Danchin, O. Bârzu, A.M. Gilles, J. Biol. Chem. 271 (1996) 2856–2862.

[47] J. Monod, J. Wyman, J.P. Changeux, J. Mol. Biol. 12 (1965) 88–118.

[48] T.S. Balganesh, P.M. Alzari, S.T. Cole, Trends Pharmacol. Sci. 29 (2008) 576–581.